Dynamical properties of a particle in a time-dependent double-well potential

2004 J. Phys. A: Math. Gen. 37 8949

(http://iopscience.iop.org/0305-4470/37/38/004)

INSTITUTE OF PHYSICS PUBLISHING JOURNAL OF PHYSICS A: MATHEMATICAL AND GENERAL

J. Phys. A: Math. Gen. **37** (2004) 8949–8968 PII: S0305-4470(04)82564-2

Dynamical properties of a particle in a time-dependent double-well potential

Edson D Leonel and P V E McClintock

Department of Physics, Lancaster University, Lancaster LA1 4YB, UK

Received 25 June 2004
Published 8 September 2004
Online at stacks.iop.org/JPhysA/37/8949
doi:10.1088/0305-4470/37/38/004

Abstract

Some chaotic properties of a classical particle interacting with a time-dependent double-square-well potential are studied. The dynamics of the system is characterized using a two-dimensional nonlinear area-preserving map. Scaling arguments are used to study the chaotic sea in the low-energy domain. It is shown that the distributions of successive reflections and of corresponding successive reflection times obey power laws with the same exponent. If one or both wells move randomly, the particle experiences the phenomenon of Fermi acceleration in the sense that it has unlimited energy growth.

PACS numbers: 05.45.-a, 05.45.Ac, 05.45.Pq, 05.45.Tp

(Some figures in this article are in colour only in the electronic version.)

1. Introduction

The dynamics of systems interacting with time-dependent potentials has received close attention in theoretical and experimental physics over many years. In quantum systems, one interesting question is the tunnelling time through a potential barrier [1]. It is well known that it depends on the energy of the particle and the height of the potential, but the situation becomes much more complicated [2] when the height of the barrier is time-dependent. Considerable effort has been devoted to trying to understand such systems, including numerical studies of the transmission probability spectrum in a driven triple diode in the presence of a periodic external field [3], photon-assisted tunnelling through a $GaAs/Al_xGa_{1-x}As$ quantum dot induced by a microwave external frequency [4], sequential tunnelling in a superlattice induced by an intense electric field [5], transmission above a quantum well considering the effect of possible capture into a bound state in the well due to dissipation [6] and the probability of tunnelling in the presence of friction in Josephson junction circuits [7].

For a classical particle interacting with a time-dependent barrier some notable results are presented in [8, 9]. The main result of these latter papers is that the traversal time, i.e. the length of time that the particle spends before crossing the barrier, obeys a power law. This is a good indication of sensitivity to initial conditions. The problem of a particle interacting with

one, two and finally an infinite chain of synchronized oscillating square wells was studied in [10]. The authors showed that, for one oscillating well, the particle is not chaotically scattered since topological chaos is not observed for such a case but that chaotic scattering is, however, observed for two oscillating wells. For the case of an infinite chain of oscillating square wells they showed that, although there is an intricate and complex dynamics, a chaotic orbit does not have unlimited energy gain. This is closely related to the fact that the phase space presents invariant spanning curves. A different version of this problem considering a classical particle interacting with an infinite box of potential that contains one oscillating square well was discussed in [11] using a formalism that could be interpreted as equivalent to studying the problem of a particle interacting with an oscillating square well with periodic boundary conditions; it could also be applied to the problem of an infinite chain of oscillating square wells. The authors found an abrupt transition in the Lyapunov exponent and suggested that it was due to destruction of the first invariant spanning curve and the consequent merging of different large chaotic regions.

It is also interesting to study problems where a classical particle interacts with a static or time-dependent multi-well potential in the presence of noise. Recent results include exact solutions for the problem of diffusion within static single and double square wells [12, 13], an introduction of external fields for a two-level system in a classical potential [14], a general solution of the problem of activated escape in periodically driven systems [15], analytical solutions for the problem of a piecewise bistable potential in the limit of low external perturbation [16], the escape flux from a multi-well metastable potential preceding the formation of quasi-equilibrium [17], activation over a randomly fluctuating barrier [18, 19], diffusion across a randomly fluctuating barrier [20] and diffusion of a particle in a piecewise potential in the presence of small fluctuations of the barriers [21]. The main result of [21] is that the flux of particles through the barrier may either increase or decrease, a result that is independent of the frequency of the oscillations.

The well-known billiards problems are closely related. They consist basically of quantum or classical particles confined within closed boundaries with which they undergo elastic collisions [22–26], producing a variety of behaviours. Depending on the boundary and the control parameters, as well as on the initial conditions, it is possible to observe integrability, non-integrability and ergodicity. The main question with a time-dependent boundary is whether or not the system exhibits the phenomenon of Fermi acceleration [27]. A more detailed discussion of this very interesting question together with specific examples can be found in [28] where the authors proposed the following conjecture: '*chaotic dynamics of a billiard with fixed boundary is a sufficient condition for the Fermi acceleration in the system when a boundary perturbation is introduced*'.

In this paper we study the problem of a particle within an infinite box of potential that contains two oscillating square wells. We will concentrate on the problem of non-synchronized oscillation, although some results for the synchronized case will also be discussed. The dynamics of this problem is analysed using a two-dimensional nonlinear area-preserving map in energy and time variables. We focus our attention on the chaotic low energy domain, characterizing it by use of Lyapunov exponents. We also derive a scaling relation for the variance of the average energy in the chaotic sea at low energy. Depending on the energy, the particle may stay trapped in one well for some interval of time. We show that the time that the particle remains trapped in the well, also called the *reflection time*, obeys a distribution fitted by a power law that has the same exponent for both wells. This distribution is observed only for chaotic orbits located below the first invariant spanning curve. In a similar way, we have observed that for very specific values of the energy, the particle can exhibit the phenomenon of *resonance* in which it exits the well with the same energy as it had on entry. As we will see,

the introduction of random fluctuations in the depths of one or both wells confers unlimited energy growth on the particle.

The paper is organized as follows: in section 2, we describe in full detail all the steps used to construct the map. We present in section 3 our results for the deterministic version of this problem, while section 4 discusses the stochastic model. Finally, we summarize and make our concluding remarks in section 5.

2. The model with periodic oscillations

We consider the problem of a classical particle moving inside an infinite box of potential that contains two oscillating square wells. It could be related directly to mesoscopic systems [3] with time-dependent potentials [3, 6] with the square wells representing the conduction band for a heterostructure of $GaAs/Al_xGa_{1-x}As$ while the time-dependent potential could represent the electron–phonon interaction [29]. Furthermore, the formalism used to derive the scaling relation for the chaotic low energy region in this problem could be very useful and directly applicable to billiards problems. Such a formalism was recently applied to the careful investigation of the chaotic sea in the Fermi–Ulam accelerator model [30].

The problem relates to a typical one-dimensional system and may be described using the Hamiltonian $H(x, p, t) = p^2/2m + V(x, t)$. Here $V(x, t)$ describes the potential within which the particle must remain, which can be written as

$$V(x,t) = \begin{cases} \infty & \text{if } x \leqslant 0 \text{ and } x \geqslant l + a + L, \\ d_1 \sin(\omega_1 t) & \text{if } 0 < x < l, \\ V_0 & \text{if } l \leqslant x \leqslant l + a, \\ d_2 \sin(\omega_2 t) & \text{if } l + a < x < l + a + L, \end{cases}$$

where d_1 and d_2 are the amplitudes of oscillation of wells I and II respectively, l and L are their widths and a is the width of the constant potential V_0. Each well oscillates independently with its own frequency, ω_1 or ω_2. The potential $V(x, t)$ is shown schematically in figure 1. We choose to describe the dynamics of this problem using a map T that gives, respectively, the new total energy and the corresponding time when the particle enters well I, i.e. $(E_{n+1}, t_{n+1}) = T(E_n, t_n)$. Although it is explicit that the Hamiltonian is time-dependent and the energy of the particle is not constant, we will show that the map describing the dynamics of this system is area-preserving.

2.1. Map derivation

We now describe in detail the steps used in the construction of the map. We adopt the same general procedures [9] recently applied [31] to the problem of a time-modulated barrier. Suppose that the particle is at $x = l$ travelling to the left with total energy $E_n = K_n + V_0$ at time $t = t_n$. As it enters well I, it experiences an abrupt change in its kinetic energy, and the new value is given by $K'_n = E_n - d_1 \sin(\omega_1 t_n)$. Inside well I, the particle travels with constant velocity $v'_n = \sqrt{2[E_n - d_1 \sin(\omega_1 t_n)]/m}$ because there are no potential gradients. It undergoes an elastic collision with the wall at $x = 0$, and is reflected back. The time taken by the particle in travelling the distance $2l$ is $t'_n = 2l/v'_n$. When it arrives at $x = l$ again, it will escape from well I only if $E'_n = K'_n + d_1 \sin[\omega_1(t_n + t'_n)] > V_0$. If $E'_n \leqslant V_0$, the particle is reflected inside well I, travels the distance $2l$ again, and so on. It will escape from well I only when the following condition is satisfied:

$$E'_n = K'_n + d_1 \sin[\omega_1(t_n + it'_n)] > V_0. \tag{1}$$

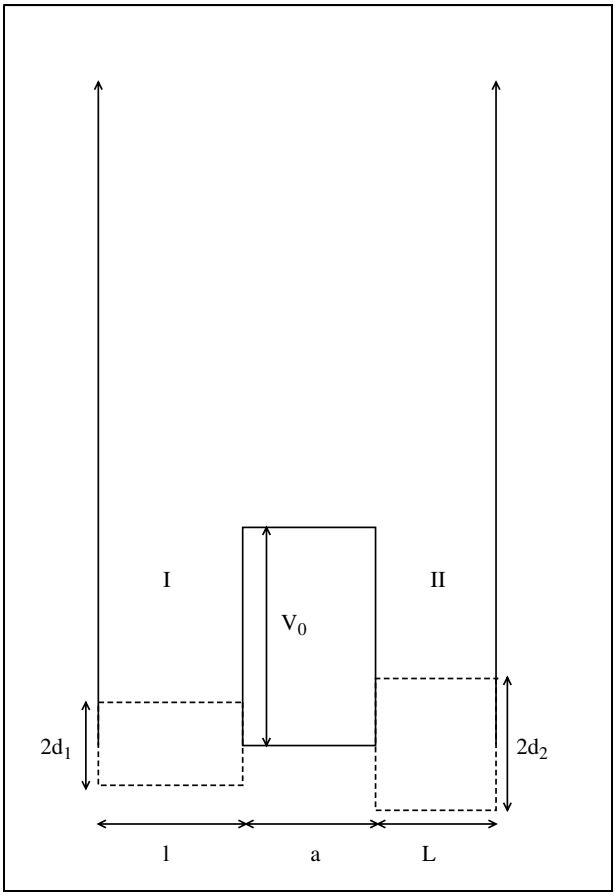

Figure 1. Sketch of the potential $V(x,t)$. The zero of x is in the bottom left-hand side corner.

Here, i is the smallest integer number that makes equation (1) true. When the particle escapes from well I, it again experiences an abrupt change in its kinetic energy, which becomes $K''_n = E'_n - V_0$. The particle then travels above the barrier with a constant velocity $v''_n = \sqrt{2K''_n/m}$ until it reaches the entrance to well II. The time spent in this way above the barrier is $t''_n = a/v''_n$. On entry to well II, the particle again suffers an abrupt change in its kinetic energy and the new relation is $K'''_n = E'_n - d_2 \sin[\omega_2(t_n + it'_n + t''_n)]$. The velocity of the particle inside the well II is $v'''_n = \sqrt{2K'''_n/m}$. When it reaches the right-hand side wall at $x = l + a + L$, it experiences an elastic collision and is reflected backwards at the same velocity. So the time spent by the particle in travelling the distance $2L$ is $t'''_n = 2L/v'''_n$. The particle will escape from well II if $E_{n+1} = K'''_n + d_2 \sin[\omega_2(t_n + it'_n + t''_n + t'''_n)] > V_0$. But if $E_{n+1} \leqslant V_0$, the particle will be reflected again inside well II, travel the distance L and, after suffering another elastic collision, will be reflected back again. It will escape from well II only if the following condition is fulfilled:

$$E_{n+1} = K'''_n + d_2 \sin[\omega_2(t_n + it'_n + t''_n + jt'''_n)] > V_0, \tag{2}$$

where j is the smallest integer for which equation (2) is true. Escaping from well II, the particle travels the distance a with velocity $v'^v_n = \sqrt{2(E_{n+1} - V_0)/m}$ in time $t'^v = a/v'^v$ until it reaches

the entrance of well I. The total time thus expended is $t_{n+1} = t_n + it'_n + t''_n + jt''' + t'^v$, so that the map T can be written as

$$T : \begin{cases} E_{n+1} = K'''_n + d_2 \sin[\omega_2(t_n + it'_n + t''_n + jt'''_n)], \\ t_{n+1} = t_n + it'_n + t''_n + jt''' + t'^v. \end{cases} \tag{3}$$

Because of the way in which the map was derived, there are an excessive number of control parameters, 8 in total, including l, L, a, ω_1, ω_2, d_1, d_2 and V_0. It is much more convenient to rewrite the map (3) in terms of dimensionless parameters, retaining only those that are relevant and effective. We use both normalized energy $e_n = E_n/V_0$ and normalized amplitudes $\delta_1 = d_1/V_0$ and $\delta_2 = d_2/V_0$ of oscillation of the bottoms of the wells. A practical measure of time could be by counting the number of oscillations of well I, so that we can define the phase $\phi_n = \omega_1 t_n$. We define the ratio of the frequencies as $r = \omega_2/\omega_1$. It is also interesting to define the following parameter:

$$N_c = \sqrt{\frac{m}{2V_0}}\frac{2l}{\tau_1}, \tag{4}$$

where $\tau_1 = 2\pi/\omega_1$ is the oscillation period of well I. The parameter N_c then gives us the number of oscillations of well I during the length of time in which the particle travels distance $2l$ inside it at constant kinetic energy $K = V_0$, in the absence of oscillations. Using these new variables, the map T can be rewritten as

$$T : \begin{cases} e_{n+1} = e_n - \delta_1 \sin(\phi_n) + \delta_1 \sin(\phi_n + i\Delta\phi_a) - \delta_2 \sin[r(\phi_n + i\Delta\phi_a + \Delta\phi_b)] \\ \qquad + \delta_2 \sin[r(\phi_n + i\Delta\phi_a + \Delta\phi_b + j\Delta\phi_c)], \\ \phi_{n+1} = \phi_n + i\Delta\phi_a + \Delta\phi_b + j\Delta\phi_c + \Delta\phi_d, \end{cases} \tag{5}$$

where the auxiliary variables are given by

$$\Delta\phi_a = \frac{2\pi N_c}{\sqrt{e_n - \delta_1 \sin(\phi_n)}}, \qquad \Delta\phi_b = \frac{a}{l}\frac{\pi N_c}{\sqrt{e'_n - 1}},$$

$$\Delta\phi_c = \frac{L}{l}\frac{2\pi N_c}{\sqrt{e'_n - \delta_2 \sin[r(\phi_n + i\Delta\phi_a + \Delta\phi_b)]}},$$

$$\Delta\phi_d = \frac{a}{l}\frac{\pi N_c}{\sqrt{e_{n+1} - 1}},$$

i is the smallest integer for which equation (6) is true,

$$e'_n = e_n - \delta_1 \sin(\phi_n) + \delta_1 \sin(\phi_n + i\Delta\phi_a) > 1, \tag{6}$$

and j is the smallest integer number for which equation (7) is true,

$$e_{n+1} = e'_n - \delta_2 \sin[r(\phi_n + i\Delta\phi_a + \Delta\phi_b)] + \delta_2 \sin[r(\phi_n + i\Delta\phi_a + \Delta\phi_b + j\Delta\phi_c)] > 1. \tag{7}$$

This map is area-preserving because it possesses the property that $\det J = 1$, where J is its Jacobian matrix. Using these variables the map now has six dimensionless and effective control parameters, namely δ_1, δ_2, N_c, r, a/l and L/l.

The case of synchronized oscillations ($r = 1$) of equal amplitude ($\delta_1 = \delta_2$) for symmetrical wells ($L/l = 1$) has already been studied [10, 11]. For the special case where the driving is also in-phase, the system must be related to the problem of a time-modulated barrier [8, 9]

(see also [31] for recent results) because the relative movement of the different parts of the potential is then identical. As we will see, however, it is also of interest to investigate the dynamical properties in the more general cases that arise where the oscillations may be of unequal amplitude, not necessarily synchronized, and where the wells may be asymmetrical as well as symmetrical.

3. Numerical results

We now present and discuss our numerical results for the model defined in section 2. The first step is to choose appropriate control parameters and to start investigating the corresponding dynamical properties. We will consider first the symmetrical case and then, secondly, the asymmetrical one.

3.1. The symmetrical case

The symmetrical case consists basically in analysing the system specified by $a/l = L/l = 1$, such that each well and the barrier (see figure 1) are of the same width. Before choosing the value of the control parameter N_c, let us first discuss its physical significance. As originally defined (see equation (4)), it gives information about the frequency of oscillation of well I, and we can rewrite it in a more appropriate form as $N_c = t_c/\tau_1$. The time $t_c = 2l\sqrt{m/(2V_0)}$ gives the interval within which the particle travels the distance $2l$ with kinetic energy $K = V_0$. Related to this time, we can define a characteristic frequency $\omega_c = 2\pi/t_c$. Using such a relation, and a similar one for the period τ_1, the control parameter N_c can be written as $N_c = \omega_1/\omega_c$. In this section, we will consider $N_c = G$ with $G = (\sqrt{5}-1)/2$, sometimes referred to as the golden mean [32]. Using this value of N_c, we obtain that $\omega_1 = 0.618\ldots\omega_c$, characterizing the fact that well I oscillates with a frequency that is low compared to ω_c. Having defined the control parameters, we now construct the phase space for this model. Figure 2 shows the phase spaces for (*a*) $r = 2$ and (*b*) $r = 3$ with a fixed amplitude of oscillation $\delta_1 = \delta_2 = 0.25$. They exhibit a very rich hierarchy of behaviours including KAM islands, invariant spanning curves and chaotic seas. We also see that variation of the control parameter r influences the shape of the phase space directly, changing the positions of the invariant spanning curves and KAM islands. An immediate consequence is that the shape of the chaotic sea is also modified. We will use the Lyapunov exponent to characterize the chaotic sea.

It is well known that the Lyapunov exponent quantifies the average exponential rate of expansion or contraction of nearby initial conditions in the phase space. In this sense, negative exponents mean convergence of two slightly different initial conditions, whereas a positive Lyapunov exponent implies their divergence. If two initial conditions diverge exponentially in time, the system presents a chaotic component and the orbit is said to be chaotic. Periodic or quasi-periodic behaviour is characterized by negative Lyapunov exponents. We use the algorithm of triangularization proposed by Eckmann and Ruelle [33] to evaluate the Lyapunov exponents. They are defined as

$$\lambda_j = \lim_{n\to\infty} \sum_{k=1}^{n} \frac{1}{n} \ln|\Lambda_j^k|, \quad j = 1, 2,$$

where Λ_j^k are the eigenvalues of $M = \prod_{k=1}^{n} J_k(e_k, \phi_k)$ and J_k is the Jacobian matrix evaluated on the orbit (e_k, ϕ_k). In order to calculate the eigenvalues of M, we use the fact that J can be written as the product $J = \Theta T$, where Θ is an orthogonal matrix and T is a triangular one.

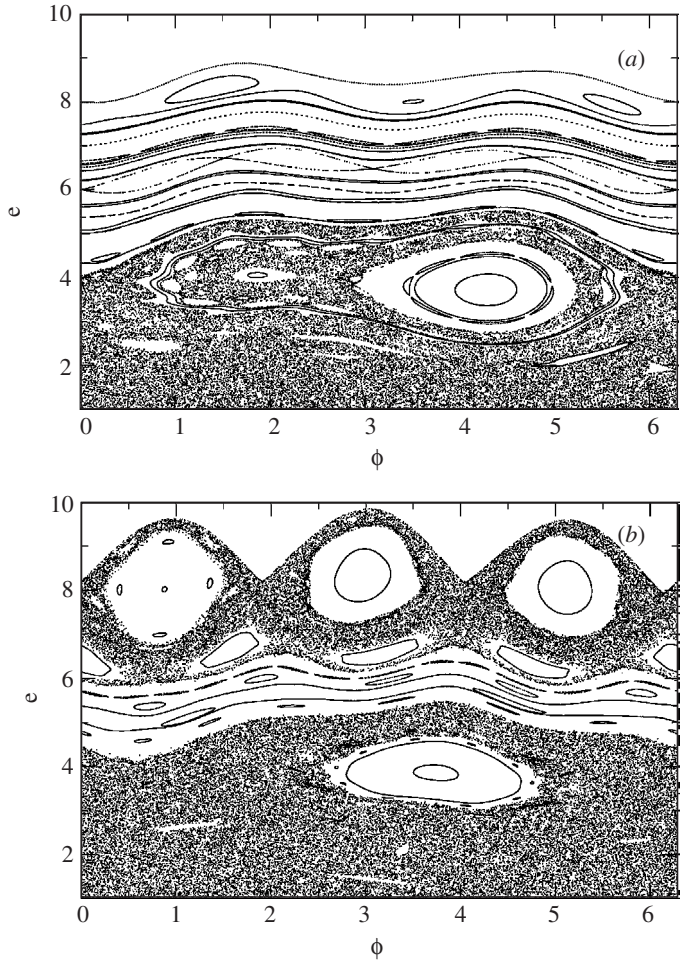

Figure 2. Phase space for the map T. The control parameters used were $a/l = L/l = 1$, $N_c = G$, $\delta_1 = \delta_2 = 0.25$, with (*a*) $r = 2$; and (*b*) $r = 3$.

We now define the elements of these matrices as

$$\Theta = \begin{pmatrix} \cos(\theta) & -\sin(\theta) \\ \sin(\theta) & \cos(\theta) \end{pmatrix}, \qquad T = \begin{pmatrix} T_{11} & T_{12} \\ 0 & T_{22} \end{pmatrix}.$$

Introducing the identity operator, we rewrite $M = J_n J_{n-1} \ldots J_2 \Theta_1 \Theta_1^{-1} J_1$, and thus define $\Theta_1^{-1} J_1 = T_1$. The product $J_2 \Theta_1$ defines a new matrix J_2^*. As a next step, we may then write $M = J_n J_{n-1} \ldots J_3 \Theta_2 \Theta_2^{-1} J_2^* T_1$. The same procedure yields $T_2 = \Theta_2^{-1} J_2^*$. The problem is thus reduced to the evaluation of the diagonal elements of T_i : T_{11}^i, T_{22}^i. Using the Θ and T matrices, we find the eigenvalues of M, given by

$$T_{11} = \frac{j_{11}^2 + j_{21}^2}{\sqrt{j_{11}^2 + j_{21}^2}}, \qquad T_{22} = \frac{j_{11} j_{22} - j_{12} j_{21}}{\sqrt{j_{11}^2 + j_{21}^2}}.$$

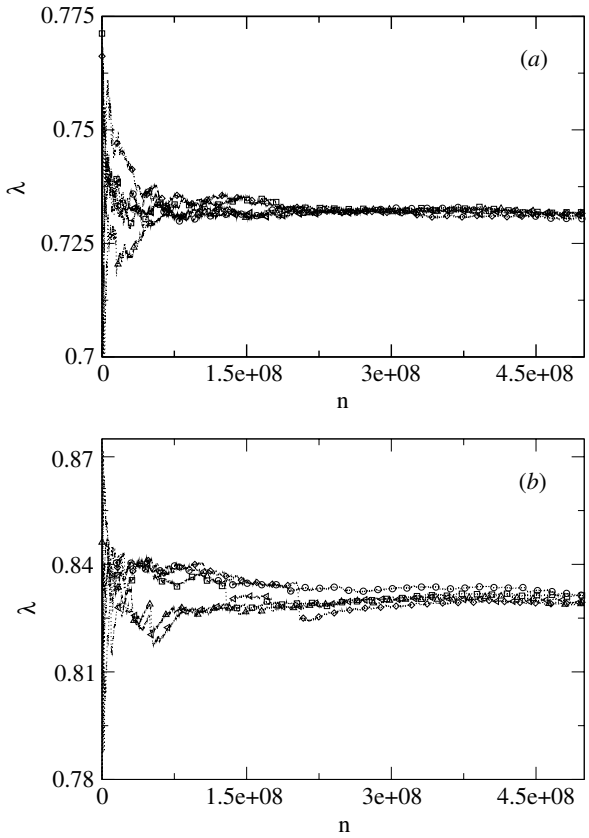

Figure 3. Asymptotic convergence of the positive Lyapunov exponent for the chaotic sea. The control parameters used were $a/l = L/l = 1$, $N_c = G$, $\delta_1 = \delta_2 = 0.25$ with (*a*) $r = 2$; and (*b*) $r = 3$.

We can then evaluate the Lyapunov exponent using the relation

$$\lambda_j = \lim_{n\to\infty} \sum_{k=1}^{n} \frac{1}{n} \ln|T_j^k|, \quad j = 1, 2.$$

The Lyapunov exponents possesses the property $\lambda_1 = -\lambda_2$ because the map T is area-preserving. Figure 3 shows the convergence of the positive Lyapunov exponent from five different initial conditions for the chaotic low energy regions shown in figure 2. Each initial condition was iterated 5×10^8 times to guarantee that the asymptotic value has been reached. The ensemble average of the five samples is: (a) $\lambda = 0.733 \pm 0.001$ and (b) $\lambda = 0.831 \pm 0.002$. We also obtain the behaviour of the positive Lyapunov exponent for the chaotic low energy region as a function of r, as shown in figure 4 for control parameters $a/l = L/l = 1$, $N_c = G$ and $\delta_1 = \delta_2 = 0.25$. Because of the change in the shape of the chaotic sea caused by variation of r, and in particular the position of the first invariant spanning curve, the asymptotic convergence of the positive Lyapunov exponent requires progressively longer runs in order to approach its asymptotic value as r increases. Equivalently, with a fixed maximum iteration number $n_{\max} = 5 \times 10^8$, the error bars for large values of r are bigger than for those for small r.

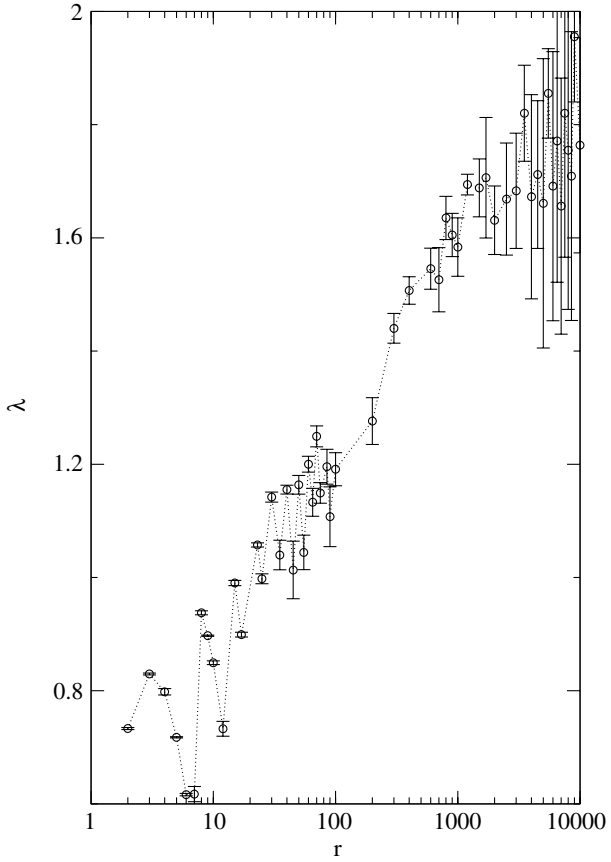

Figure 4. Positive Lyapunov exponent, λ as a function of r for the chaotic sea. The control parameters used were $a/l = L/l = 1$, $N_c = G$ and $\delta_1 = \delta_2 = 0.25$.

Let us now discuss some scaling properties for this model in the region related to the chaotic sea. We choose to characterize the behaviour in terms of the variance of the average energy, which we will refer as the *roughness* ω [34]. The procedure adopted here has already been used to characterize the chaotic low energy region of the Fermi–Ulam accelerator model [30] and to investigate scaling present in the chaotic sea for a time-modulated barrier [31]. Given the large number of control parameters present in this model, we will consider the following parameters to be fixed: $a/l = L/l = 1$; $\delta_1 = \delta_2 = 0.25$; $r = G$ (unsynchronized case). We then study the behaviour of the roughness as a function of the parameter N_c. To define the roughness we must first consider the average of the energy over the orbit generated from one initial condition

$$\bar{e}(n, N_c) = \frac{1}{n}\sum_{i=0}^{n} e_i, \tag{8}$$

and then evaluate the interface width around this average energy. We can thus define the roughness formally, considering an ensemble of B different initial conditions, as

$$\omega(n, N_c) \equiv \frac{1}{B}\sum_{j=1}^{B}\left(\sqrt{\overline{e^2}_j(n, N_c) - \bar{e}_j^2(n, N_c)}\right). \tag{9}$$

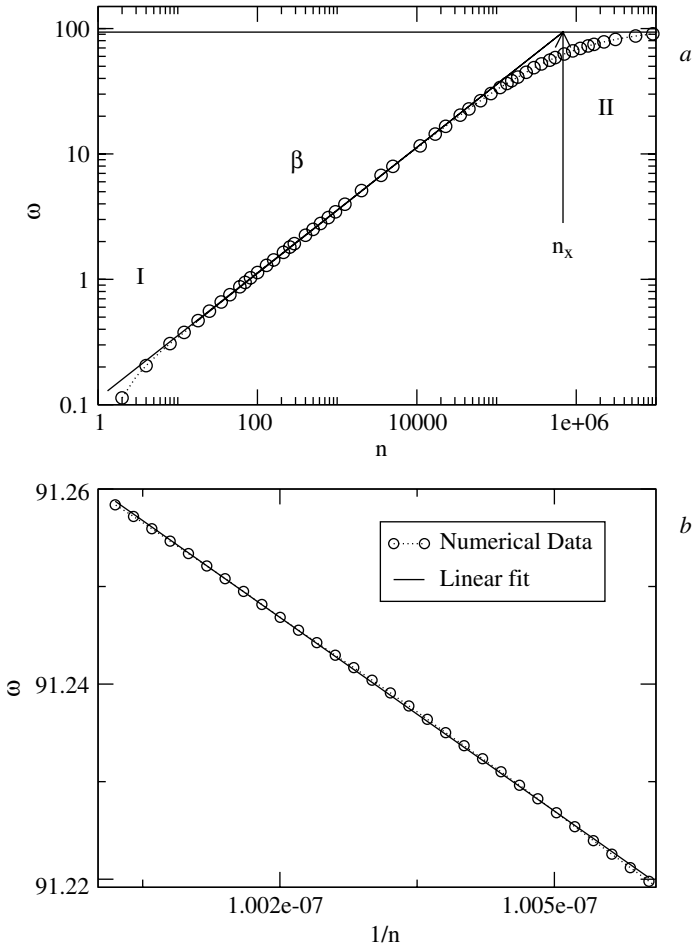

Figure 5. (*a*) Roughness evolution for an ensemble of 5000 different initial phases and the same initial energy $e_0 = 1.001$, all of them leading to chaotic behaviour. (*b*) Procedure used to extrapolate the roughness after application of the transformation $n \to 1/n$. The values of control parameters were $a/l = L/l = 1$, $\delta_1 = \delta_2 = 0.25$, $r = G$ and $N_c = 3000$.

An ensemble of initial conditions is used to smooth the roughness evolution, for which a typical curve is shown in figure 5(*a*); it was constructed by fixing the initial energy at $e_0 = 1.001$ and then ensemble-averaging 5000 different initial phases in the interval $\phi_0 \in [0, 2\pi)$; all of them gave rise to chaotic behaviour. The main idea of averaging over the initial phases is to analyse the asymptotic dynamics starting for the same initial energy, but considering a large number (in principle) of allowed positions to the bottom of well I. We can see in figure 5(*a*) that there are two different regimes of behaviour. After a very brief initial transient, the roughness grows according to a power law and then, as the iteration number increases, the roughness eventually bends towards the direction of a saturation regime that is obtained only for a long enough iteration number (see below for the details used to extrapolate the saturation of the roughness). The changeover from growth to convergence on saturation is characterized by a crossover iteration number n_x. It is well known that the chaotic sea is limited by the first invariant spanning curve which, in a sense, plays the role of a boundary limiting the size of

the chaotic sea. As an immediate consequence of this limitation, the roughness saturates. As the control parameter N_c increases, however, the position of the first invariant spanning curve changes. For the range of N_c over scaling in the roughness is investigated, an increase in N_c implies a rise in the position of the first invariant spanning curve so that, as a consequence, the roughness saturates at a higher value. We can then start to characterize the roughness scaling, supposing that the following points hold:

(i) After the brief initial transient, the roughness grows as a function of iteration number according to

$$\omega(n, N_c) \propto n^{\beta}. \tag{10}$$

This growth can be seen in region I of figure 5. β is called the growth exponent. Equation (10) is valid for $n \ll n_x$.

(ii) As the iteration number increases, the roughness reaches saturation, as can be seen in region II of figure 5. The behaviour of the roughness within the saturation regime follows the equation

$$\omega_{sat}(N_c) \propto N_c^{\alpha}, \tag{11}$$

where α is the roughening exponent. Equation (11) is only valid for $n \gg n_x$.

(iii) The crossover iteration number n_x that tells us when the roughness growth slows and saturation is being approached is given by

$$n_x(N_c) \propto N_c^{z}, \tag{12}$$

where z is called the dynamical exponent.

We now summarize the procedure adopted to obtain the saturation value. Even for our maximum iteration number ($n \approx 500 n_x$), we can see from the numerical simulations that growth of the roughness has not quite reached saturation. But if we choose to increase the maximum iteration number even more, this carries the disadvantage of leading to very much longer simulations. We therefore take the option of finding the saturation value by extrapolation. We apply the transformation $n \to 1/n$ for the iteration number, which is applicable because the saturation grows slowly and linearly for sufficiently large values of n, yielding

$$\omega(n, N_c) = \omega_{sat}(N_c) + \frac{\text{const.}}{n}. \tag{13}$$

Considering the case of $n \to \infty$, it is easy to see that equation (13) gives us that $\omega(n, N_c) \to \omega_{sat}(N_c)$, which may be obtained after doing a linear fit to the results. The procedure is illustrated in figure 5(b).

Next we discuss how to obtain the exponents α and z. The intercept of the power law (see figure 5(a)) with the linear coefficient obtained from equation (13) gives the crossover iteration number n_x. The exponents α and z are then obtained from the graphs of $n(N_c)$ and $\omega_{sat}(N_c)$ as shown in figure 6. Applying the power-law fit, we find that $\alpha = 0.632(5)$ and $z = 1.26(1)$. Obtaining β by averaging over all curves in the range of figure 6, we find $\beta = 0.500(2)$.

Having found the exponents, we can then proceed to collapse the roughness curves onto a universal plot. As the first step, we take the ratio $\omega(N_c)/\omega_{sat}(N_c)$. This procedure relocates all curves to the same saturation value, as shown in figure 7(b). The second step is to relocate all the curves to the same crossover iteration number, which is done by taking the ratio n/n_x as shown in figure 7(c).

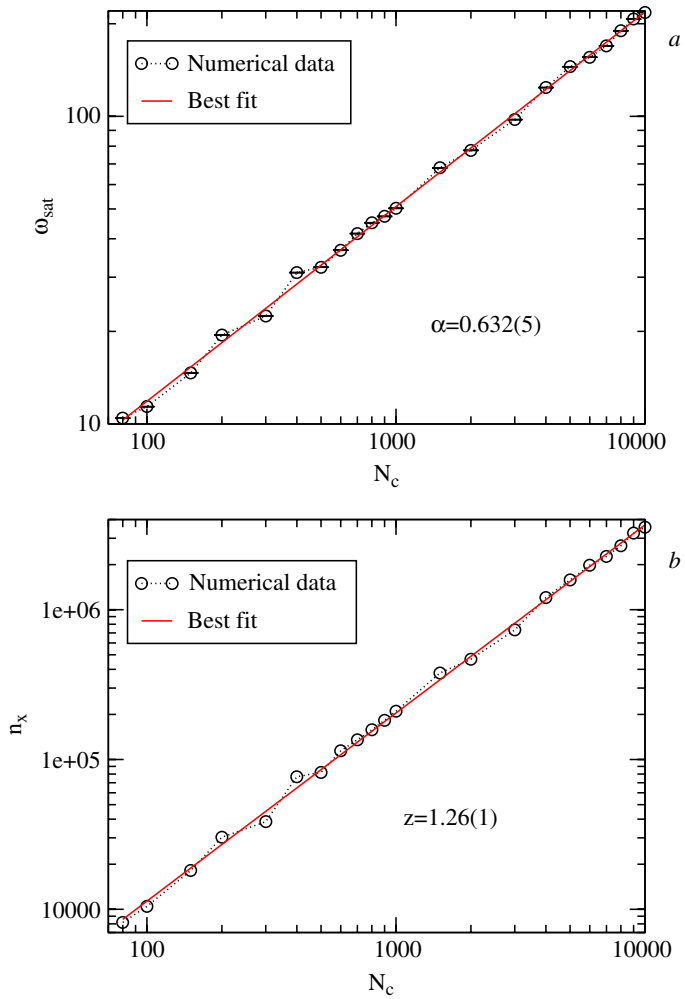

Figure 6. (*a*) Roughness saturation ω_{sat} and (*b*) crossover iteration number n_x as functions of the control parameter N_c. A power-law fit gives us that $\alpha = 0.632(5)$ and $z = 1.26(1)$.

The success of this procedure for obtaining a universal plot for the roughness allows us to describe it using the following scaling function:

$$\omega(n, N_c) = \zeta\omega(\zeta^b n, \zeta^c N_c), \tag{14}$$

where ζ is the scaling factor. We can then choose $\zeta = n^{-1/b}$ and rewrite equation (14) as

$$\omega(n, N_c) = n^{-1/b}\omega_1(n^{-c/b}N_c).$$

The function $\omega_1(n^{-c/b}N_c) = \omega(1, n^{-c/b}N_c)$ is assumed constant for $n \ll n_x$. Considering equation (10) we obtain

$$n^{-1/b} = n^{\beta},$$

and $\beta = -1/b$. From our numerical simulations we have $\beta = 0.500(2)$.

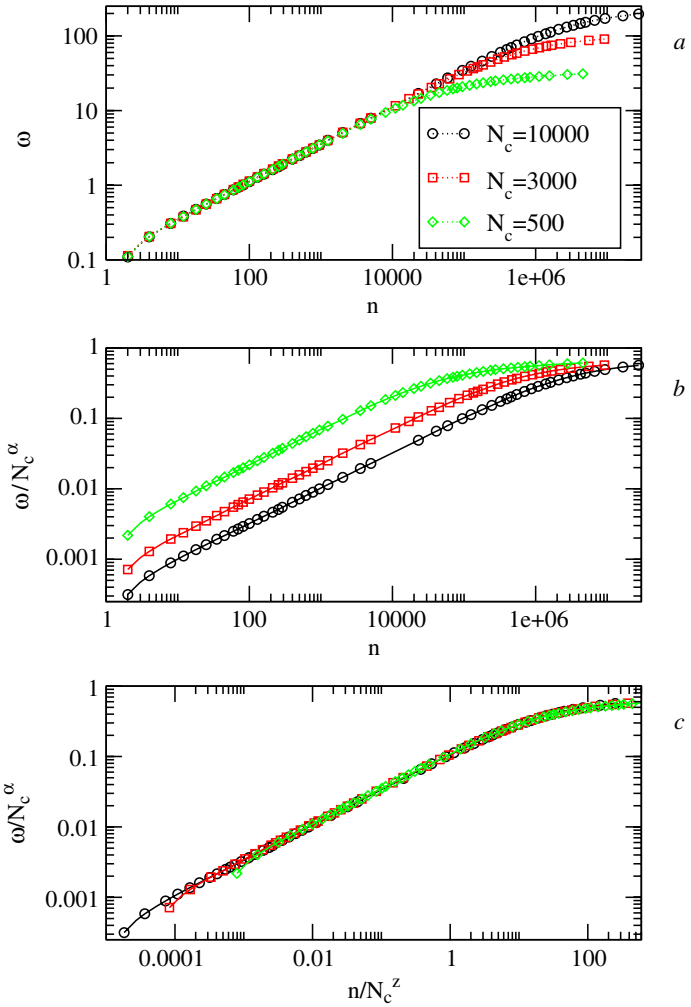

Figure 7. (*a*) Roughness evolution for different values of N_c. (*b*) Collapse of the curves onto the same saturation value. (*c*) Collapse of the curves onto the same saturation value and same crossover iteration number.

Our second choice is $\zeta = N_c^{-1/c}$ and we have that

$$\omega(n, N_c) = N_c^{-1/c}\omega_2(N_c^{-b/c}n),$$

where the function $\omega_2(N_c^{-b/c}n) = \omega(1, N_c^{-b/c}n)$ is supposed to be constant for $n \gg n_x$. Using equation (11) we obtain that

$$N_c^{-1/c} = N_c^{\alpha},$$

with $\alpha = -1/c$.

Using the two previous relations together with the scaling factor and the corresponding relations for the exponents b and c, it is easy to show that the exponents α, β and z are mutually connected by the following relationship:

$$z = \frac{\alpha}{\beta}. \tag{15}$$

Evaluating equation (15) with our numerical results for α and β, we find that $z = 1.264(5)$, which is gratifying close to the result obtained in figure 6(b).

3.2. The asymmetrical case

We now discuss a resonance phenomenon that manifests in the chaotic sea. It depends specifically on the energy of the particle immediately after it enters a well, and it may occur in either of the wells (see also [31] for a fuller discussion of resonances in the problem of a time modulated barrier). Entering the well, the corresponding range of energy where the resonance can take place is: (a) well I, $e \in [e^{\rm I}_{min}, e^{\rm I}_{max}]$ and (b) well II, $e \in [e^{\rm II}_{min}, e^{\rm II}_{max}]$, where $e^{\rm I}_{min} = 1 - \delta_1$, $e^{\rm I}_{max} = 1 + \delta_1$, $e^{\rm II}_{min} = 1 - \delta_2$ and $e^{\rm II}_{max} = 1 + \delta_2$. The resonances can be determined directly from the length of time that the particle spends travelling inside each well. For well I, this time is

$$\Delta\phi_a = \frac{2\pi N_c}{\sqrt{e_n - \delta_1 \sin(\phi_n)}},$$

and for well II it is

$$\Delta\phi_c = \frac{L}{l}\frac{2\pi N_c}{\sqrt{e'_n - \delta_2 \sin[r(\phi_n + i\Delta\phi_a + \Delta\phi_b)]}}.$$

If either of these times is a multiple of 2π, the particle will not remain trapped within the corresponding well. From the range of energy within the relevant well, we can estimate the number of oscillations, the resonance energy, and the time of flight. The corresponding maximum and minimum values for the number of oscillations are given by: (a) well I, $k^{\rm I}_{max} = N_c/\sqrt{e^{\rm I}_{min}}$ and $k^{\rm I}_{min} = N_c/\sqrt{e^{\rm I}_{max}}$; (b) well II, $k^{\rm II}_{max} = (L/l)(N_c/\sqrt{e^{\rm II}_{min}})$ and $k^{\rm II}_{min} = (L/l)(N_c/\sqrt{e^{\rm II}_{max}})$. After obtaining the range of k values, the respective resonance energies for the two wells are

$$e^{\rm I}_k = \frac{N_c^2}{k^2} \quad \text{and} \quad {\rm e}^{\rm II}_k = \left(\frac{L}{l}\right)^2 \frac{N_c^2}{k^2}.$$

To illustrate the occurrence of such resonances, we choose to characterize the synchronized case ($r = 1$) and asymmetric case $a/l = 1$, $L/l = 2.5$ by different amplitudes of oscillation, $\delta_1 = 0.25$, $\delta_2 = 0.35$ for $N_c = 15G$. The latter value of N_c gives $\omega_1 = 9.270\ldots\omega_c$ and we have that the bottom of well I oscillates in a moderate range compared to ω_c. Table 1 lists the corresponding numbers of oscillations, resonance energies, and flight times for both wells I and II. It is also expected that near to the resonance energies, the probability of observing a successive reflection inside the well, i.e. sufficient condition for the particle to stay temporally trapped, should be quite low. To provide evidence of such behaviour, we obtained numerically the distribution of successive reflections energies as shown in figure 8. We stress that, exactly at resonance, the particle has zero probability of being trapped in the well; the corresponding energies are indicated in figure 8. However, if the particle has low but non-resonant energy, it could be trapped in the well transiently, suffering successive reflections until it has sufficient energy to escape. We now consider this case.

We discussed in section 2 how, depending on the energy of the particle as it enters the well, it can stay trapped there while suffering successive reflections. After some interval of time, however, after satisfying some specific conditions, it will exit the well, and evolve inside the system (mainly in chaotic behaviour) until it again becomes trapped, not necessarily in the same well. In this way, we can characterize the distribution of successive reflections as well as the length of time during which the particle stays trapped in the well. It is expected

Table 1. Resonance energies and flight times inside both, wells I and II for the control parameters $r = 1$, $a/l = 1$, $L/l = 2.5$, $\delta_1 = 0.25$, $\delta_2 = 0.35$ and $N_c = 15G$.

k	e_k	$\Delta\phi_{a,c}$
Well I		
9	1.0610...	56.5486...
10	0.8594...	62.8318...
Well II		
20	1.3428...	125.6637...
21	1.2180...	131.9468...
22	1.1097...	138.2300...
23	1.0153...	144.5132...
24	0.9325...	150.7964...
25	0.8594...	157.0796...
26	0.7945...	163.3628...
27	0.7368...	169.6460...
28	0.6851...	175.9291...

that very long times (i.e. large number of successive reflections) should be observed less commonly than short times (small numbers of successive reflections). To characterize such behaviour, we choose the following combination of control parameters: the asymmetric case ($a/l = 10$), ($L/l = 3$) considering non-synchronized oscillations ($r = G$ and $N_c = 15G$) of differing amplitude $\delta_1 = 0.25$ and $\delta_2 = 0.35$. Figure 9 shows the distributions of successive reflections, P_n, and the corresponding successive reflection times, P_t, for well I (a similar result is in fact also observed for well II). The analysis of figure 9 allows us to describe such distributions as $P_n \propto t^{\gamma_n}$ and $P_t \propto t^{\gamma_t}$. After performing a power-law fit, we obtain for well I that $\gamma_n = -2.99(1)$ and $\gamma_t = -3.00(2)$. A similar analysis for well II yields $\gamma_n = -3.00(1)$ and $\gamma_t = -3.01(1)$. So, we can conclude that $\gamma_n = \gamma_t \approx -3$. It is of interest that such an exponent value has also been reported for other, different, one-dimensional models, so that these results may be indicative of some kind of universality. The same exponent was found numerically for the distribution of traversal times over a time-modulated barrier [8, 9] and for a well beside a time-dependent barrier [31], and accounted for analytically in the case of a particle moving within a random well [11].

4. The stochastic model

Next, we describe the model with stochastic perturbations. Suppose that the potential can be written as $V(x,t) = V(x)\,f_k(t)$ with $k = 1, 2$ to indicate wells I and II, respectively. The function $f_k(t)$ may be periodic (periodic model) or randomly varying, according to choice. If the function is random, it gives a set of completely uncorrelated random numbers uniformly distributed between $[-1, 1]$ with the property that $\langle f_k \rangle = 0$. Using this formalism, the map T is written as

$$T: \begin{cases} e_{n+1} = e_n - \delta_1 f_1(t_n) + \delta_1 f_1(t_n + i\Delta t_a) - \delta_2 f_2[r(t_n + i\Delta t_a + \Delta t_b)] \\ \qquad\quad + \delta_2 f_2[r(t_n + i\Delta t_a + \Delta t_b + j\Delta t_c)], \\ t_{n+1} = t_n + i\Delta t_a + \Delta t_b + j\Delta t_c + \Delta t_d, \end{cases}$$

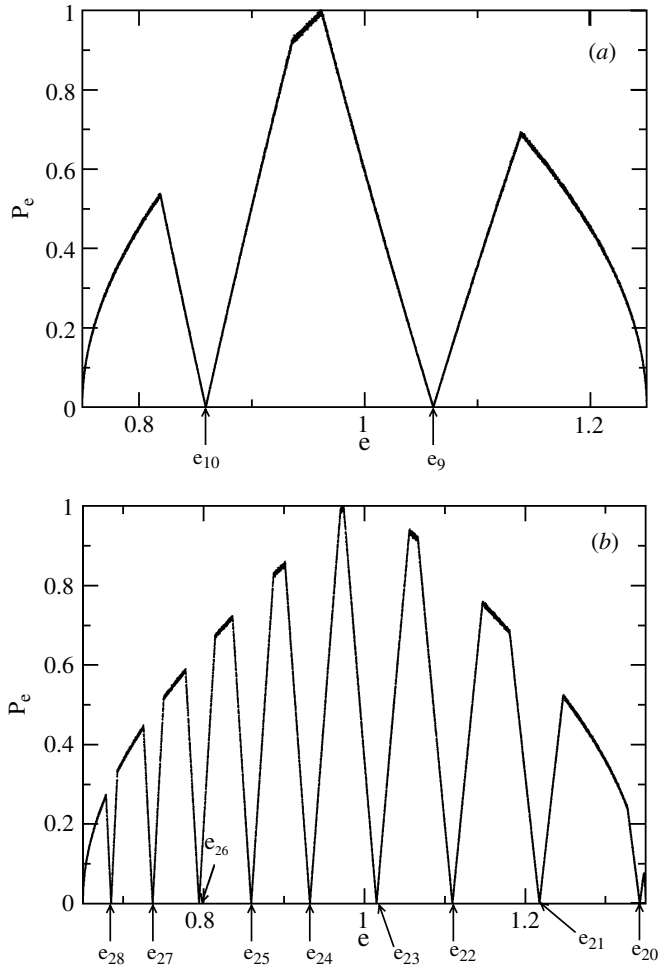

Figure 8. Normalized distribution of successive reflection energies for the control parameters $r = 1$, $a/l = 1$, $L/l = 2.5$, $\delta_1 = 0.25$, $\delta_2 = 0.35$ and $N_c = 15G$ for (*a*) well I and (*b*) well II.

where the auxiliary variables are given by

$$\Delta t_a = \frac{2\pi N_c}{\sqrt{e_n - \delta_1 f_1(t_n)}}, \qquad \Delta t_b = \frac{a}{l}\frac{\pi N_c}{\sqrt{e'_n - 1}},$$

$$\Delta t_c = \frac{L}{l}\frac{2\pi N_c}{\sqrt{e'_n - \delta_2 f_2[r(t_n + i\Delta t_a + \Delta t_b)]}},$$

$$\Delta t_d = \frac{a}{l}\frac{\pi N_c}{\sqrt{e_{n+1} - 1}},$$

i is the smallest integer number for which the following equation is true:

$$e'_n = e_n - \delta_1 f_1(t_n) + \delta_1 f_1(t_n + i\Delta t_a) > 1,$$

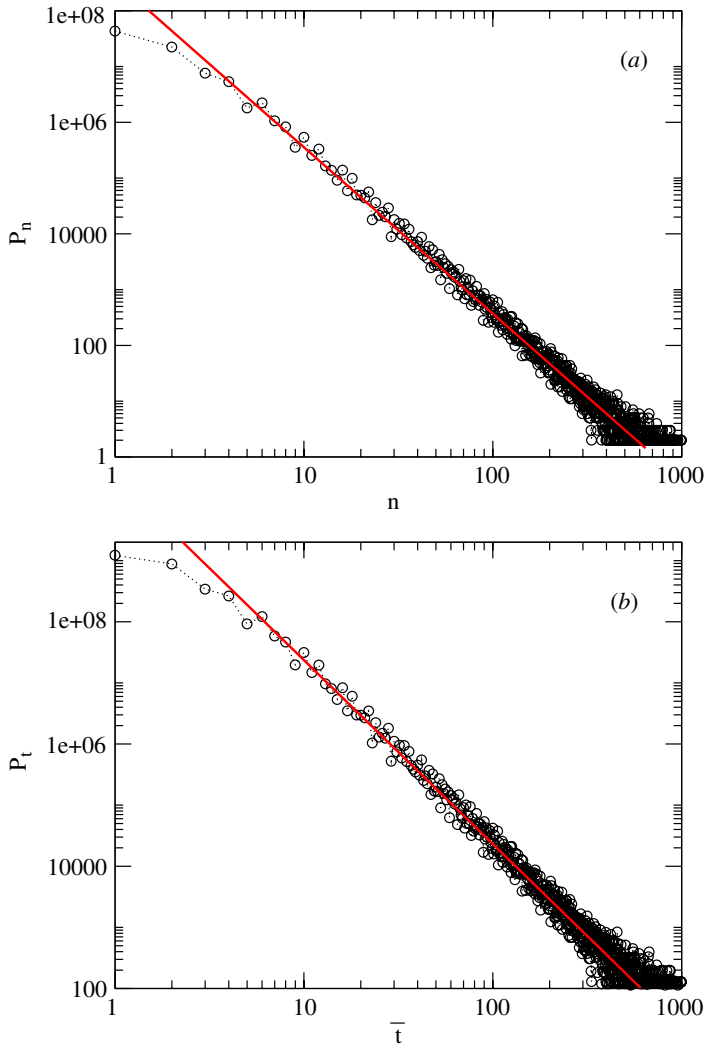

Figure 9. (*a*) Distribution of successive reflections, P_n, and (*b*) successive reflection times P_t obtained for well I. The values of control parameters used were $a/l = 10$, $L/l = 3$, $r = G$, $N_c = 15G$, $\delta_1 = 0.25$ and $\delta_2 = 0.35$. A power-law fit gives us that $\gamma_n = -2.99(1)$ and $\gamma_t = -3.00(2)$.

and j is the smallest integer number that makes true the equation

$$e_{n+1} = e'_n - \delta_2 f_2[r(t_n + i\Delta t_a + \Delta t_b)] + \delta_2 f_2[r(t_n + i\Delta t_a + \Delta t_b + j\Delta t_c)] > 1.$$

We consider three different kinds of stochastic perturbation to this system:

(1) Well I is periodic and well II moves randomly. In this situation, $f_1(t) = \sin(t)$ and $f_2(t)$ give uncorrelated random numbers.
(2) Well II is periodic and well I moves randomly. With these conditions, $f_1(t)$ gives uncorrelated random numbers and $f_2(t) = \sin(rt)$.
(3) Wells I and II both move randomly, i.e. $f_1(t)$ and $f_2(t)$ both give uncorrelated random numbers, and in addition, functions $f_1(t)$ and $f_2(t)$ are mutually uncorrelated.

The introduction of the stochastic perturbation affects directly the complex structure of the phase space. In particular, for the range of control parameters used, it is possible to observe unlimited energy growth in the time evolution of the particle. To make evident this behaviour, we evaluate the following observables:

$$\bar{e} = \frac{1}{B}\sum_{i=1}^{B}\left[\frac{1}{n}\sum_{j=1}^{n} e_{j,i}\right], \qquad \bar{t} = \frac{1}{B}\sum_{i=1}^{B}\left[\frac{1}{n}\sum_{j=1}^{n} t_{j,i}\right]. \tag{16}$$

The sum over n gives the average over the orbit, while the sum over B gives the average over the ensemble of initial conditions. Although a calculation for just one initial condition is sufficient to provide evidence for such growth, averaging over an ensemble of initial conditions makes the energy curve smoother and much easier to characterize. Figure 10 shows the behaviour of $\bar{e}(n)$ and $\bar{e}(\bar{t})$. The control parameters used were $a/l = L/l = 1$, $r = G$, $\delta_1 = \delta_2 = 0.25$ and $N_c = G$. Similar results can be obtained for other combinations of control parameters. We use an ensemble of 10 000 different initial conditions, starting with an initial energy $e_0 = 1.001$ and different initial seeds for the random number generator. Each initial condition was iterated 10^7 times. The analysis of figure 10 allows us to describe the growth of the energy as (a) $\bar{e} \propto n^{\delta_n}$ and (b) $\bar{e} \propto \bar{t}^{\delta_t}$. Considering the case in which well I behaves randomly while well II is periodic, our results show that $\delta_n = 0.498(3)$ and $\delta_t = 0.647(2)$ (as in figure 10). For the case where well I is periodic and well II behaves randomly, we obtain that $\delta_n = 0.496(4)$ and $\delta_t = 0.644(7)$. Finally, considering the case where both wells behave randomly, a power-law fit gives $\delta_n = 0.497(4)$ and $\delta_t = 0.648(3)$. We can see that both exponents are robust, in the sense that they are independent of which well (I, or II, or both) is behaving randomly. The averages of the latter three exponents are given by $\bar{\delta}_n = 0.497(4)$ and $\bar{\delta}_t = 0.646(4)$. It is especially gratifying that the exponent $\bar{\delta}_n$ has the same value as that obtained from a random walk, given that the dynamics is essentially the same. In an attempt to account for the difference between the exponents $\bar{\delta}_n$ and $\bar{\delta}_t$ we point out that, during a given interval, a particle with high energy can iterate many more times within a well than a particle with low energy. The authors of [28] conjectured that Fermi acceleration should be observed for a billiard with a time-dependent boundary if the corresponding version for a fixed boundary presents chaotic components. However, we can conclude that for the system studied in the present paper (see also [11] and [31] for comparable results in other systems) which exhibits chaotic behaviour under a time-dependent (periodic) perturbation, Fermi acceleration is observed only after the introduction of random (stochastic) motion to the time-dependent potential.

5. Final remarks and conclusions

We have studied the problem of a classical particle inside an infinite box of potential that contains two time-dependent square wells. We describe this problem via the formalism of a discrete map, considering two types of time dependence: (i) periodic and (ii) stochastic. For the periodic dependence we discuss results for both the symmetrical and asymmetrical cases, as well as for both the synchronized and unsynchronized cases. We concentrate on the chaotic low-energy region, which we characterize in terms of Lyapunov exponents. We derive a scaling relation for the variance of the average velocity (roughness) and show that the critical exponents obey an analytical relationship. In the low-energy region, the particle may stay temporarily trapped in the time-dependent well. We have shown that the distributions of successive reflection numbers and successive reflection times obey power laws with the same exponent. The particle may also experience the phenomenon of resonance, i.e. it may

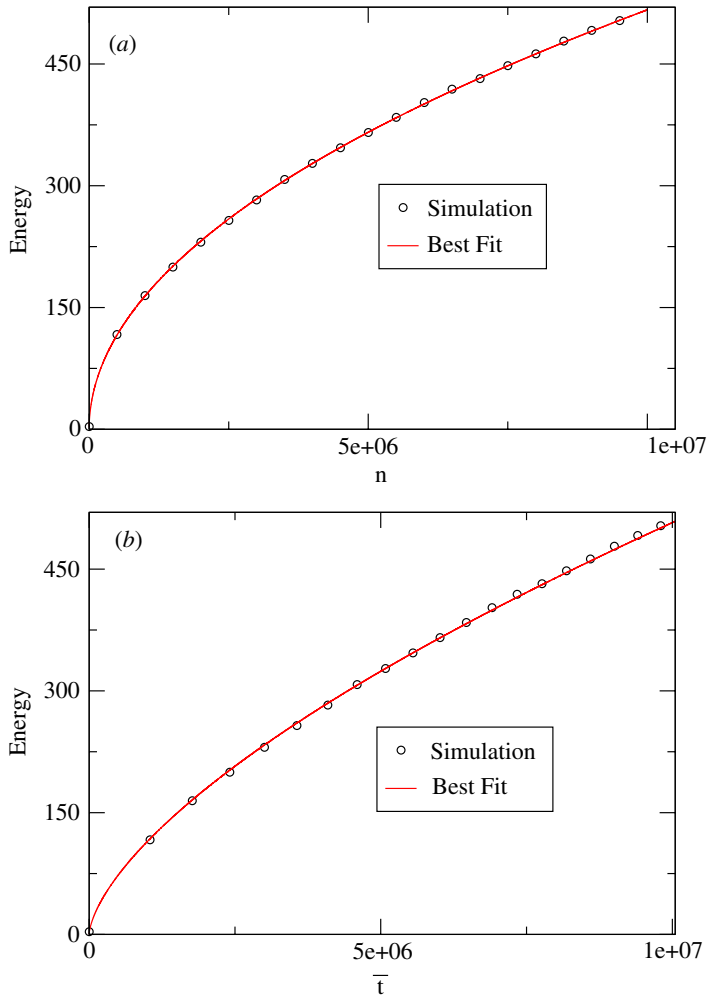

Figure 10. Behaviour of the average energy as a function of (a) iteration number n and (b) average time $\bar{t}$ for the case where $f_1(t)$ is random and $f_2(t)$ is periodic. The control parameters used were $N_c = r = G$, $\delta_1 = \delta_2 = 0.25$, $a/l = L/l = 1$. A power-law fit gives that $\delta_n = 0.498(3)$ and $\delta_t = 0.647(2)$.

exit the well with the same energy as it had when it entered. For the case in which one or both wells move randomly, we have shown that the particle exhibits growth in velocity and correspondingly in kinetic energy. Such a behaviour is a clear evidence of the Fermi acceleration phenomenon.

Acknowledgments

This research was supported by a grant from Conselho Nacional de Desenvolvimento Científico CNPq, Brazilian agency. The numerical results were obtained at the Centre for High Performance Computing in Lancaster University. The work was supported in part by the Engineering and Physical Sciences Research Council (UK).

References

[1] Cohen-Tannoudji C, Diu B and Laloë F 1977 *Quantum Mechanics* vol I (New York: Wiley)
Gasiorowicz S 1974 *Quantum Physics* (New York: Wiley)
[2] Büttiker M and Landauer R 1982 *Phys. Rev. Lett.* **49** 1739
[3] Wagner M 1998 *Phys. Rev.* B **57** 11899
[4] Kouwenhoven L P, Jauhar S, Orenstein J, McEuen P L, Nagamune Y, Motohisa J and Sakaki H 1994 *Phys. Rev. Lett.* **73** 3443
[5] Guimarães P S S, Keay B J, Kaminski J P, Allen S J Jr, Hopkins P F, Gossard A C, Florez L T and Harbison J P 1993 *Phys. Rev. Lett.* **70** 3792
[6] Cai W, Hu P, Zheng T F, Yudanin B and Lax M 1990 *Phys. Rev.* B **41** 3513
[7] Caldeira A O and Leggett A J 1981 *Phys. Rev. Lett.* **46** 211
[8] Mateos J L and José J V 1998 *Physica* A **257** 434
[9] Mateos J L 1999 *Phys. Lett.* A **256** 113
[10] Luna-Acosta G A, Orellana-Rivadeneyra G, Mendoza-Galván A and Jung C 2001 *Chaos Solitons Fractals* **12** 349
[11] Leonel E D and da Silva J K L 2003 *Physica* A **323** 181
[12] Berdichevsky V and Gitterman M 1996 *Phys. Rev.* E **53** 1250
[13] Berdichevsky V and Gitterman M 1996 *J. Phys. A: Math. Gen.* **29** 1567
[14] Berdichevsky V and Gitterman M 1999 *Phys. Rev.* E **59** R9
[15] Dykman M I, Golding B, McCann L I, Smelyanskiy V N, Luchinsky D G, Mannella R and McClintock P V E 2001 *Chaos* **11** 587
[16] Berdichevsky V and Gitterman M 1996 *J. Phys. A: Math. Gen.* **29** L447
[17] Arrayás M, Kaufman I Kh, Luchinsky D G, McClintock P V E and Soskin S M 2000 *Phys. Rev. Lett.* **84** 2556
[18] Iwaniszewski J 2003 *Phys. Rev.* E **68** 027105
[19] Iwaniszewski J, Kaufman I Kh, McClintock P V E and McKane A J 2000 *Phys. Rev.* E **61** 1170
[20] Iwaniszewski J 1996 *Phys. Rev.* E **54** 3173
[21] Berdichevsky V and Gitterman M 1999 *Phys. Rev.* E **60** 7562
[22] Karner G 1994 *J. Stat. Phys.* **77** 867
[23] Seba P 1990 *Phys. Rev.* A **41** 2306
[24] Tsang K Y and Ngai K L 1997 *Phys. Rev.* E **56** R17
[25] Berry M V 1981 *Eur. J. Phys.* **2** 91
[26] Robnik M and Berry M V 1985 *J. Phys. A: Math. Gen.* **18** 1361
[27] Fermi E 1949 *Phys. Rev.* **75** 1169
[28] Loskutov A, Ryabov A B and Akinshin L G 2000 *J. Phys. A: Math. Gen.* **33** 7973
[29] Cai W, Zheng T F, Hu P, Yudanin B and Lax M 1989 *Phys. Rev. Lett.* **63** 418
[30] Leonel E D, McClintock P V E and da Silva J K L 2004 *Phys. Rev. Lett.* **93** 14101
[31] Leonel E D and McClintock P V E 2004 *Phys. Rev.* E **70** 16214
[32] Lichtenberg A J and Lieberman M A 1992 *Regular and Chaotic Dynamics, Appl. Math. Sci.* vol 38 (New York: Springer)
[33] Eckmann J-P and Ruelle D 1985 *Rev. Mod. Phys.* **57** 617
[34] Barabási A-L and Stanley H E 1985 *Fractal Concepts in Surface Growth* (Cambridge: Cambridge University Press)